

# Exploiting the transit timing capabilities of *Ariel*

Luca Borsato · Valerio Nascimbeni · Giampaolo Piotto · Gyula Szabó

Received: 2020 June 30 / Accepted: 2021 March 15

**Abstract** The Transit Timing Variation (TTV) technique is a powerful dynamical tool to measure exoplanetary masses by analysing transit light curves. We assessed the transit timing performances of the *Ariel* Fine Guidance Sensors (FGS1/2) based on the simulated light curve of a bright, 55 Cnc, and faint, K2-24, planet-hosting star. We estimated through a Markov-Chain Monte-Carlo analysis the transit time uncertainty at the nominal cadence of 1 second and, as a comparison, at a 30 and 60-s cadence. We found that at the nominal cadence *Ariel* will be able to measure the transit time with a precision of about 12s and 34s, for a star as bright as 55 Cnc and K2-24, respectively. We then ran dynamical simulations, also including the *Ariel* timing errors, and we found an improvement on the measurement of planetary masses of about 20-30% in a K2-24-like planetary system through TTVs. We also simulated the conditions that allow us to detect the TTV signal induced by an hypothetical external perturber within the mass range between Earth and Neptune using 10 transit light curves by *Ariel*.

**Keywords** *Ariel* · transit times · TTV · planetary dynamics

## 1 Introduction

The Transit Time Variation (TTV) technique is a powerful tool to discover multi-bodies orbiting around a star, and can be used to characterise exoplanetary systems by measuring changes in the orbital period due to gravitational interaction between planets (Agol et al., 2005; Holman and Murray, 2005; Miralda-Escudé, 2002). The amplitude of the TTV effect is greatly boosted if the planets are near a mean-motion resonance (MMR, Agol et al., 2005; Holman and Murray, 2005), allowing us to infer, in particular configurations, even the presence of an exoplanet in the Earth-mass regime. The *Kepler* mission (Borucki et al., 2011), and its extension *Kepler/K2* (Howell et al., 2014), demonstrated the potentiality of this technique, able to characterise planets also for stars too faint for a spectroscopy analysis and radial velocity measurement. Some examples of the application of the TTV technique on multiple planet systems are: Kepler-9 (Holman et al., 2010; Borsato et al., 2014, 2019), Kepler-11 (Lissauer et al., 2011, 2013), Kepler-88 (Nesvorný et al., 2013; Weiss et al., 2020), K2-24 (Petigura et al., 2016, 2018), and WASP-47 (Vanderburg et al., 2017; Weiss et al., 2017). A TTV can be the result of other different physical sources, e.g. star spots, oblateness of hosting star, orbital precession induced by tidal interactions, and general relativity (for a general review see Perryman, 2018), and non-physical sources such as binning or sampling of the data (e.g. Kipping, 2010a; Mazeh et al., 2013; Szabó et al., 2013; Price and Rogers, 2014). In this work we

L. Borsato  
INAF-Osservatorio Astronomico di Padova  
Vicolo dell'Osservatorio 5, - 35122 - Padova - Italy  
E-mail: luca.borsato@inaf.it

V. Nascimbeni  
INAF-Osservatorio Astronomico di Padova  
Vicolo dell'Osservatorio 5, - 35122 - Padova - Italy

G. Piotto  
Università di Padova  
Dipartimento di Fisica e Astronomia "Galileo Galilei"  
Vicolo dell'Osservatorio 3, 35122 Padova - Italy

G. Szabó  
ELTE Eötvös Loránd University  
Gothard Astrophysical Observatory  
Szent Imre h. u. 112, Szombathely, Hungary

focus on TTV only due to gravitational interaction of exoplanets.

The European Space Agency (ESA) adopted *Ariel* (Atmospheric Remote sensing Infrared Exoplanet Large survey; Pascale et al., 2018; Pilbratt, 2019; Puig et al., 2018; Tinetti et al., 2018) as an M4 mission within the Cosmic Vision programme, and its launch is scheduled for 2028. The *Ariel* mission aims to study the atmospheres and the chemical compositions of exoplanets by surveying about 1000 transiting exoplanets through fast-cadence high-precision spectroscopy and photometry of transits, eclipses, and phase-curves in a wide spectral range from the visible (VIS,  $0.5\ \mu\text{m}$ ) to the infrared (IR,  $7.8\ \mu\text{m}$ ; detailed description in Tinetti et al., 2018; Encrenaz et al., 2018; Zingales et al., 2018; Pascale et al., 2018). The *Ariel* satellite mount two spectrometers, the *Ariel* Infrared Spectrometer (AIRS, two prism-dispersed channels that cover the band width  $1.95\text{--}3.9\ \mu\text{m}$  with  $R > 100$  and  $3.9\text{--}7.8\ \mu\text{m}$  with  $R > 30$ ) and NIRSpc (slit-less prism spectrometer with spectral resolving power  $R > 15$  in spectral range of  $1.1\text{--}1.95\ \mu\text{m}$ ), and three photometers, namely VISPhot ( $1.1\text{--}1.95\ \mu\text{m}$ ) and two *Ariel* Fine Guidance Sensors (FGS1 at  $0.6\text{--}0.8\ \mu\text{m}$  and FGS2 at  $0.8\text{--}1.11\ \mu\text{m}$ ). See Tinetti et al. (2018), Pascale et al. (2018), and Mugnai et al. (2020) for further details on *Ariel* instruments. The fast-cadence photometric data will allow us to measure the planetary transit time at precision and accuracy level of a few seconds. This is crucial to extend the temporal baseline of TTV signals of known planets in multiple-planet systems, breaking the degeneracy on doubtful dynamical solutions and improving the precision on their masses and orbital parameters (Petigura et al., 2018; Delrez et al., 2018).

In this work we present a study on the *Ariel* timing performances based on simulations of real targets (Sec. 2) and some possible science cases (Sec. 3). This analysis describes one of the possible extended uses of the *Ariel*'s Core data and it has been developed within the *Ariel* Working Group High-Precision Photometry (described in details in Szabo et al.; 2020, submitted and in Haswell 2020, in preparation).

## 2 Transit Time analysis

We simulated two science cases, modelled after the real planet hosts 55 Cnc e and K2-24 b, by analysing synthetic light curves assuming the nominal performances of FGS1 and 2. In our analysis we simultaneously fitted the light curves gathered from the two channels to get a single value of the parameters that are not dependent on wavelength, such as the  $T_0$ . We simulated photometric data at three different cadences: 1 s, that is the

nominal cadence of *Ariel* observations, 30 and 60 s as a comparison, in order to understand when the sampling cadence becomes a limiting factor for our analysis.

For both targets we estimated the expected *Ariel* photometric noise per time unit, and for each band-pass, by using the ArielRad code (Mugnai et al., 2020). This program takes into account different sources of noise, such as detector noise (dark current, gain and read-out noise), and other stationary random processes modelled as Poisson noise, i.e. photon noise, Zodiacal noise, and instrument emission). ArielRad cannot include non-stationary noise (time-correlated noise), so it includes a jitter noise as the variance at different wavelength on timescale of 1 hour, and it includes a margin noise to take into account noise uncertainties and possible time-correlated effects (about 20% on top of the photon noise, see Mugnai et al., 2020). We rescaled the noise to the actual sampling cadence and we added a noise floor of 20 ppm in quadrature (as shown in eq. 17 of Mugnai et al., 2020). This noise floor is needed to avoid to indefinitely integrate down the noise (Beichman et al., 2014; Greene et al., 2017; Mollière et al., 2017), and it is 20 ppm at every integration time (Mugnai et al., 2020). Due to the lack of time-correlated model in the noise analysis of ArielRad, we also added a linear trend (as 0.2% on the transit time scale) to the light curve to mimic the presence of systematic effects from astrophysical (e.g. stellar activity) or from instrumental sources (e.g. due to stray light or pointing effects of the satellite). We scaled the FGS2 trend as a random Gaussian with  $\sigma = 0.005$ ). We also created light curves with a quadratic term<sup>1</sup>, and scaled the FGS2 as before. We analysed the statistics of Table 4 of Holczer et al. (2016) and we found that for 92.2% of the planets (on a sample of 2339) the trend could be described by a polynomial of first order; the rest can be detrended with a second and third order polynomial (4.7% and 3.2%, respectively). So, we can assume that in most cases a linear trend is a good approximation of the out-of-transit on timescales of 2–3 transit duration. However, the measurement of the transit time and of its uncertainty is strongly affected by the sampling of the ingress and egress phases and by the symmetry of the transit model, so, the trend (and the red noise) contributes only at a second order. We decided to only fit a linear trend even if the light curve has been created with a quadratic one and a red noise term.

We modelled the transit light curve with the *batman* package (Kreidberg, 2015) and we ran a statistical anal-

<sup>1</sup> We used coefficients  $c_2 = -0.003$ ,  $c_1 = 0.002$ ,  $c_0 = 0.0$ , from high to low order.

ysis with the `emcee`<sup>2</sup> package (Foreman-Mackey et al., 2013, 2019), a Markov-Chain Monte-Carlo (MCMC) code with an affine-invariant sampler (Goodman and Weare, 2010).

Firstly, we generated the synthetic transit light curve with the physical parameters reported in Table 1. Then, for each cadence, we fitted common parameters (different parameterization with respect to Table 1) between the two filters, i.e. the stellar density in solar units ( $\rho_*$ ), the base-2 logarithm of the period ( $\log_2 P$ , used in combination with  $\rho_*$  to constraint the  $a/R_*$ ), the impact parameter<sup>3</sup> ( $b$ ), a combination of eccentricity  $e$  and argument of pericenter  $\omega$  ( $\sqrt{e} \cos \omega$ ,  $\sqrt{e} \sin \omega$ ), and the transit time ( $T_0$ ), while, for each filter, we fitted the planet to stellar radius ratio ( $k = R_p/R_*$ ), the quadratic limb-darkening (LD) coefficients,  $q_1$  and  $q_2$ , an uninformative sampling of quadratic LD  $u_1$  and  $u_2$  in the form  $q_1 = (u_1 + u_2)^2$  and  $q_2 = 0.5u_1(u_1 + u_2)^{-1}$  as suggested in Kipping (2013), a jitter factor in base-2 logarithm ( $\log_2 \sigma_{\text{jitter}}$ ), and linear trend. We selected the best (and common) parameterization of the fitting model to reduce the correlation among parameters and allowing the `emcee` code to properly, and as evenly as possible, sample the parameter space. We wanted to simulate an *Ariel* transit observation, i.e. different transit depth for each different band-pass depending on different planetary radius that corresponds to different layers of atmosphere. Given that the two FGS channels have different, almost non-overlapping, band-pass (see Figure 2 in Mugnai et al., 2020), we decided to fit different  $k$ , but we generated the synthetic light curves with a single value. We used as priors the stellar density (computed from stellar mass and radius), period  $P$ , and eccentricity reported in Table 1, and we set very tight prior if the parameter has a null error (i.e. eccentricity of 55 Cnc e). We did not apply any priors on the LD coefficients.

The `emcee` code outputs the posterior distribution of the fitted parameters from which we extract a best-fit solution and an uncertainty as the high density interval (HDI at 68.27%, equivalent of  $1-\sigma$ ) for the transit model parameters, including the most relevant here, i.e. the transit time ( $T_0$ ) and its uncertainty ( $\sigma_{T_0}$ ). As best-fit solution we compared the median, the mode<sup>4</sup>, and the

maximum likelihood estimation (MLE, as the parameter sample that maximises the likelihood within the HDI). In our cases the differences among these best-fit parameter sets are negligible (in terms of values and uncertainties) and we decided to use as representative of the best-fit solution the median of the posterior distribution, because of its symmetry with respect to the HDI. We want also to stress that finding the best-fit solution was out of the purpose of this work and we wanted to focus on the determination of the uncertainty of the parameters, mainly the  $\sigma_{T_0}$ .

## 2.1 55 Cnc e

The first case, 55 Cnc e, has been selected to assess the performances of *Ariel* on transit timing at the bright end. The magnitude and spectral type of the host star 55 Cnc ( $V = 5.95$  mag,  $M_* = 0.91 M_\odot$ ,  $R_* = 0.94 R_\odot$ ; von Braun et al., 2011) and the size of planet e,  $R_e \sim 2 R_\oplus$  (Demory et al., 2016) represent a perfect case to assess the feasibility of a solar-like star with a small transiting planet. Its transit has very short, and almost vertical, ingress and egress phases, reducing the impact of the LD effect to the timing of the transit model.

We obtained stellar and planetary parameters from von Braun et al. (2011) and Demory et al. (2016) and available through the NASA Exoplanet Archive<sup>5</sup>. We computed the coefficients of a quadratic LD-law ( $u_1$  and  $u_2$ ) fitting the ATLAS (Kurucz, 1979) and PHOENIX (Husser et al., 2013) models through the tool<sup>6</sup> developed by Espinoza and Jordán (2015). We assumed a box-shaped filter for both FGS1 and FGS2 within the spectral range of  $0.8 - 1.0 \mu\text{m}$  and  $1.05 - 1.2 \mu\text{m}$ , respectively. We adopted the values of  $u_1$  and  $u_2$  for the fitting as the average of the values computed for each combination of stellar parameters and their extremal errors for both models, obtaining:  $u_1 = 0.33$ ,  $u_2 = 0.23$  for the FGS1 and  $u_1 = 0.26$ ,  $u_2 = 0.25$  for the FGS2. We also tested LD coefficients for band  $I$  and  $J$  computed with `exofast`<sup>7</sup> (Eastman et al., 2013):  $u_1 = 0.39$ ,  $u_2 = 0.22$  for the  $I$  band and  $u_1 = 0.22$ ,  $u_2 = 0.29$  for the  $J$  band. We used the LD coefficients of  $I$  for FGS1 and those of  $J$  for FGS2 and we found no difference with the results obtained from the LD coefficients computed from the stellar models. See in Table 1 the summary of the stellar and planetary parameters used to create the synthetic light curves.

The analysis (see best-fit model for each cadence in Fig. 1) yields an estimated uncertainty in the transit

<sup>2</sup> We are aware that `emcee` code should be used with caution when space of the parameters has a number of dimension greater than 10, but it has been extensively used in exoplanet literature showing great performances in different cases. Furthermore, using a parameterization that reduces the correlation among parameters and that allows the algorithm to evenly sample the parameter space can mitigate this issue.

<sup>3</sup> In the impact parameter we taken into account the eccentricity and the argument of pericenter as in Winn (2010) and Kipping (2010b).

<sup>4</sup> As mode =  $3 \times \text{median} - 2 \times \text{mean}$

<sup>5</sup> <https://exoplanetarchive.ipac.caltech.edu/>

<sup>6</sup> <http://www.github.com/nespinoza/limb-darkening>

<sup>7</sup> <http://astroutils.astronomy.ohio-state.edu/exofast/limbdark.shtml>

**Table 1** Stellar and planetary parameters adopted in the synthetic light curves. 55 Cnc e parameters from [von Braun et al. \(2011\)](#); [Demory et al. \(2016\)](#), K2-24 b from [Petigura et al. \(2016, 2018\)](#).

Parameters	55 Cnc e	K2-24 b
$T_{\text{eff}}$ (K)	$5196 \pm 24$	$5625 \pm 60$
$\log g$ (dex)	$4.45 \pm 0.01$	$4.29 \pm 0.05$
$[Fe/H]$ (dex)	$0.31 \pm 0.04$	$0.34 \pm 0.04$
$M_*$ ( $M_{\odot}$ )	$0.91 \pm 0.02$	$1.07 \pm 0.06$
$R_*$ ( $R_{\odot}$ )	$0.94 \pm 0.01$	$1.16 \pm 0.04$
$R_p$ ( $R_{\oplus}$ )	1.91	5.4
$P$ (days)	$0.736539 \pm 0.000007$	$20.88977 \pm 0.00035$
$T_0^{(a)}$ (days)	5733.013	6905.886
$e$	0	$0.06 \pm 0.01$
$\omega$ ( $^{\circ}$ )	90	90
$i$ ( $^{\circ}$ )	83.3	89.25
FGS1		
$u_1$	0.33	0.29
$u_2$	0.23	0.25
noise (ppm/hr) <sup>(b)</sup>	12.4	54.0
FGS2		
$u_1$	0.26	0.23
$u_2$	0.25	0.26
noise (ppm/hr) <sup>(b)</sup>	5.6	43.5

<sup>(a)</sup>  $T_0$  expressed as  $\text{BJD}_{\text{TDB}} - 2450000$ . <sup>(b)</sup> Noise value from ArielRad. We added in quadrature a noise floor of 20 ppm as described in the text.

time ( $\sigma_{T_0}$ ) of 12 s, 12 s, and 14 s for cadence at 1 s, 30 s, and 60 s respectively, that is the sampling cadence for bright targets is not a limiting factor.

## 2.2 K2-24 b

The second case, K2-24 b, is a Neptune-size transiting planet in a multiple-planet system showing anti-correlated TTVs with another transiting planet (K2-24 c). The star is much fainter than 55 Cnc ( $V = 11.28$ ,  $K = 9.18$ ) with a mass and radius slightly bigger than the Sun ( $M_* = 1.07 M_{\odot}$ ,  $R_* = 1.16 R_{\odot}$ ).

We studied the transit timing performances of *Ariel* with the same two FGS channels as before and we also analysed the impact of a few *Ariel* observations on the recovering of the planetary ephemeris and on the improvement of the other orbital parameters (see Sec. 3). We used the stellar parameters from [Petigura et al. \(2018\)](#) and we computed the quadratic LD coefficients, as we did for 55 Cnc e. We found  $u_1 = 0.29$ ,  $u_2 = 0.25$  for the FGS1 and  $u_1 = 0.23$ ,  $u_2 = 0.26$  for the FGS2. We also tested LD coefficients from *exofast*:  $u_1 = 0.32$ ,  $u_2 = 0.27$  for the *I* band and  $u_1 = 0.17$ ,  $u_2 = 0.30$  for the *J* band. A summary of the stellar and planetary parameters are reported in Table 1.

In the K2-24 b case, when using LD for *I* and *J* we obtained for each cadence the same  $\sigma_{T_0}$  of 35 s. This result suggests us that in this situation we are photon

noise dominated. In the analysis with the LD from box-shaped FGS1 and 2 filters we obtained  $\sigma_{T_0}$  of 34 s, 29 s, and 32 s for cadence at 1 s, 30 s, and 60 s respectively. In both analysis the  $\sigma_{T_0}$ , obtained with only one transit, is about half the best timing uncertainty ( $\sim 78$  s) obtained with Kepler/K2 observations ([Petigura et al., 2018](#)).

We also analysed the case of K2-24 b observed by *Ariel* with only one channel, i.e. the FGS1. This could mimic the possible failure of one of the instruments, reducing the number of light curves per transit. We generated the synthetic light curve with the parameters in Table 1 with LD coefficients of FGS1 in *I* band. We repeated the analysis as before and we obtained a  $\sigma_{T_0}$  of about 53 seconds, that is still better than Kepler/K2 timing obtained from the simultaneous analysis of four transits for this target. This could be due to the high cadence photometry that is able to homogeneously sample the ingress and egress, the transit phases that have the greatest impact on determining the transit time.

## 3 Dynamical analysis

### 3.1 Impact of *Ariel* observations

K2-24 is a multiple-planet system showing anti-correlated TTVs by the transiting planet b and c, but with a poor sampling of the TTV period on K2 data ([Petigura et al., 2016, 2018](#)). This can lead to an imprecise or ambiguous

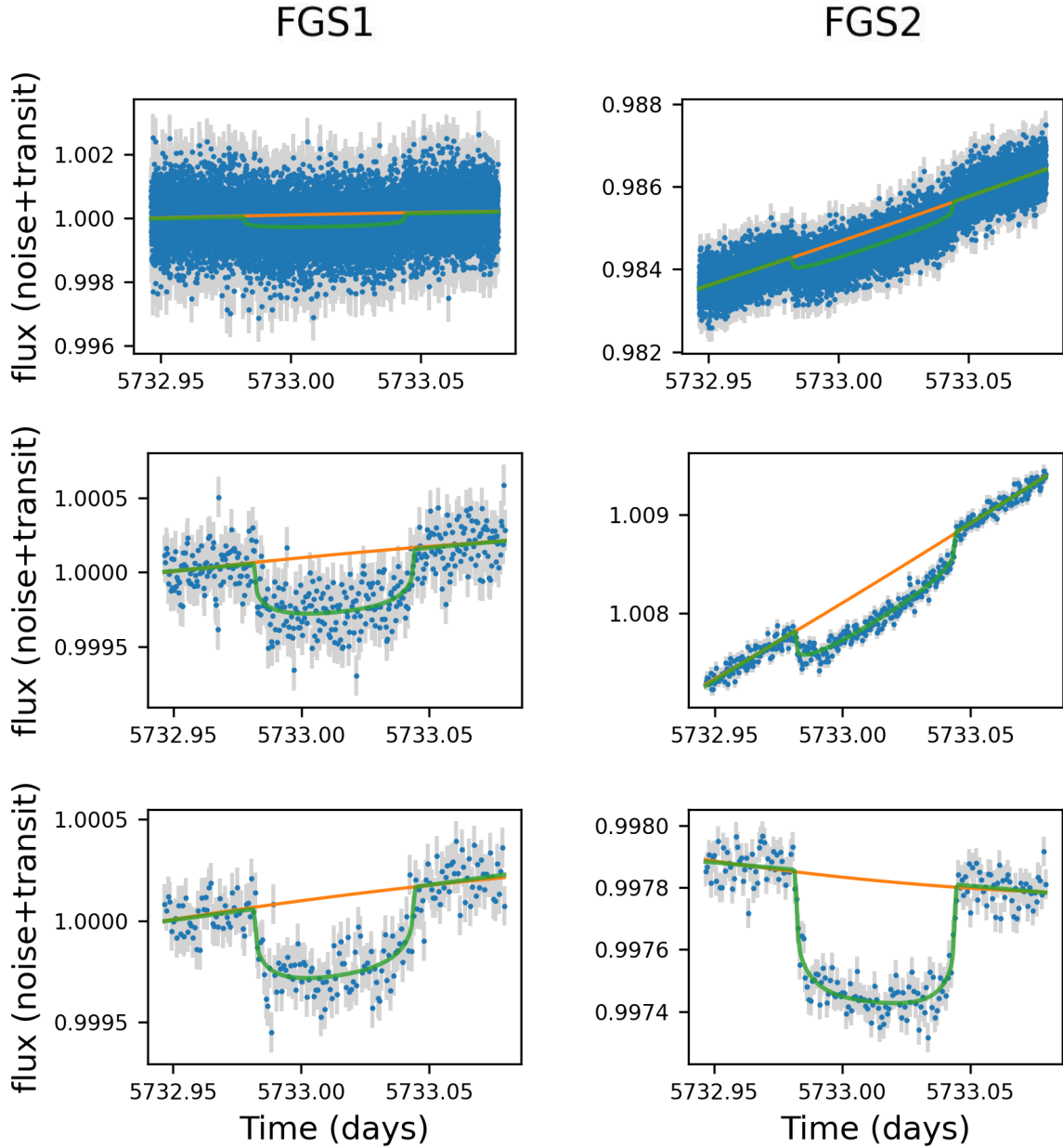


**Fig. 1** Transit light curves of 55 Cnc e with simulated *Ariel* noise (blue dots with gray error bars) and quadratic trend (orange line) along with the best-fit transit model with fitted linear trend (green line) for FGS1 (left) and FGS2 (right). First row for 1 s cadence, second and third row for 30 s and 60 s, respectively.

determination of masses and orbital parameters of the planets (see the Kepler-9 case by [Holman et al., 2010](#); [Borsato et al., 2014, 2019](#)). [Petigura et al. \(2018\)](#) found a possible candidate planet d, from the radial velocity (RV) analysis, with a mass of  $54 \pm 14 M_{\oplus}$  and a period of about 427 days.

We simulate the K2-24 system with the dynamical integrator within the TRADES code<sup>8</sup> ([Borsato et al., 2014](#); [Malavolta et al., 2017](#); [Borsato et al., 2019](#)). We

integrated the orbits for the same time range spanning the observations by Kepler/K2 and follow-up (radial velocities, RVs, and additional transits) and computed all the transit times ( $T_0$ s) and RVs within the same range. We then selected the corresponding  $T_0$ s and RVs analysed by [Petigura et al. \(2018\)](#) and we added white noise, based on the actual error bars from the same work. We used TRADES with the `emcee` module to get masses and orbital parameters from this synthetic data set and to compute the so-called “Observed - Calculated” ( $O - C$ ) plot, where the residuals of the observed  $T_0$  with respect

<sup>8</sup> <https://github.com/lucaborsato/trades>



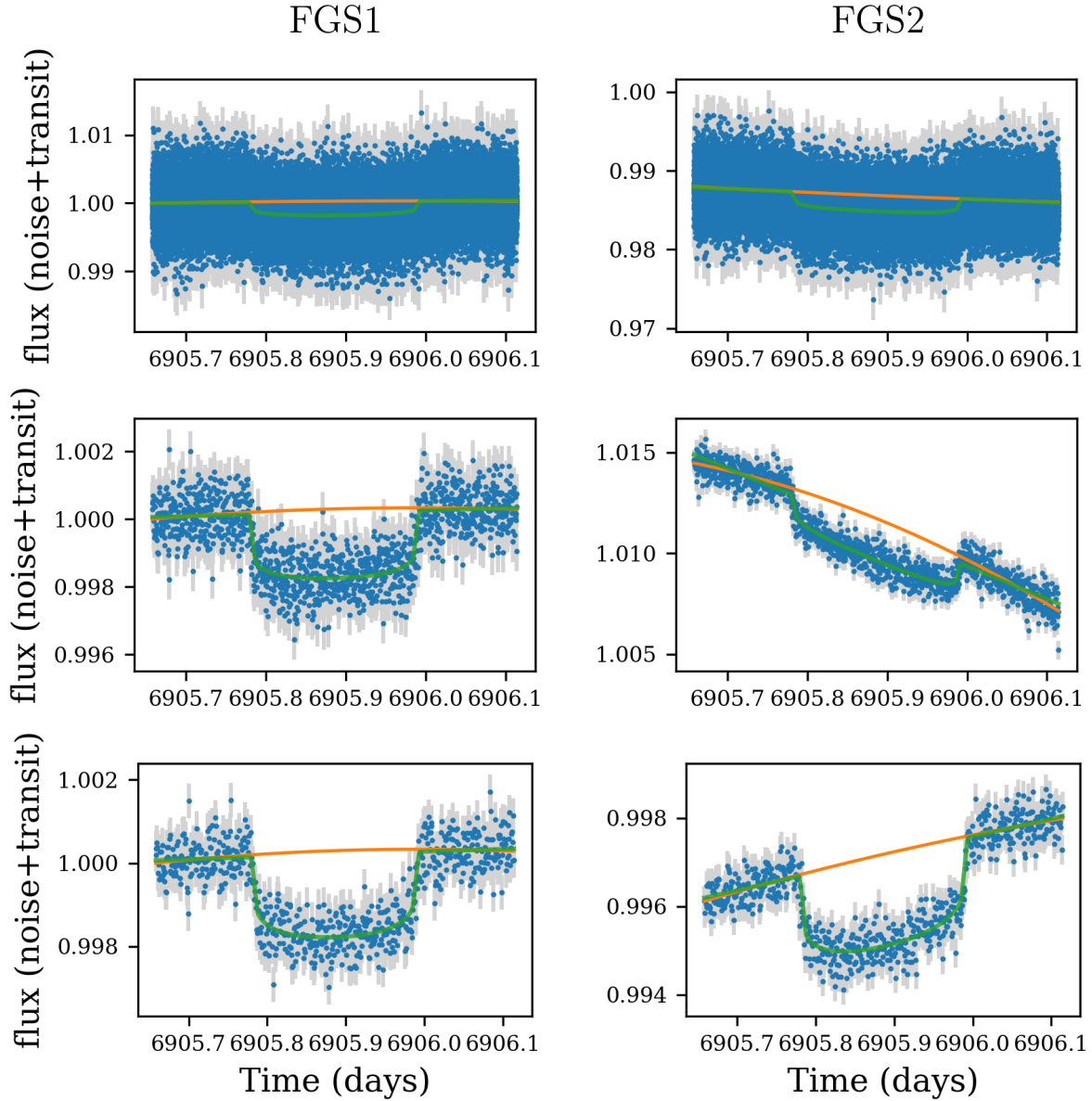


**Fig. 2** Same as in Fig. 1, but for K2-24 b.

to the reference linear ephemeris are shown as a function of time (see Fig. 3).

If we integrate for 10 years further the orbital solution obtained, we have two main effects on the prediction of the transit times. The accumulating errors of the linear ephemeris produce a shift of the transit time with respect to the predicted one. Another source of error on the transit time is due to the uncertainty on the orbital parameters of the planetary system (see. Fig. 4). In 2028, when the *Ariel* launch is supposed to take place, the shift from the linear ephemeris could lead to almost one day of uncertainty on the transit times. Even if we could recover the ephemeris, we still

have more than three hours of uncertainty on transit times due to the errors on the orbital parameters.

We simulated the K2-24 system and ran a dynamical retrieval with **TRADES+emcee** in the case of our synthetic data set with two observations with *Ariel*, one for planet b and one for c. We assumed the same error bar for the two transit times  $\sigma_{T_0} = 35$  s, that is the highest (conservative) value obtained from the previous analysis (see Sec. 2.2). We built the  $O - C$  plots (see Fig. 5) from the best-fit solution extracted from the posterior distribution and we found that just one transit per planet is enough to recover the ephemeris and to greatly improve the knowledge of orbital pa-

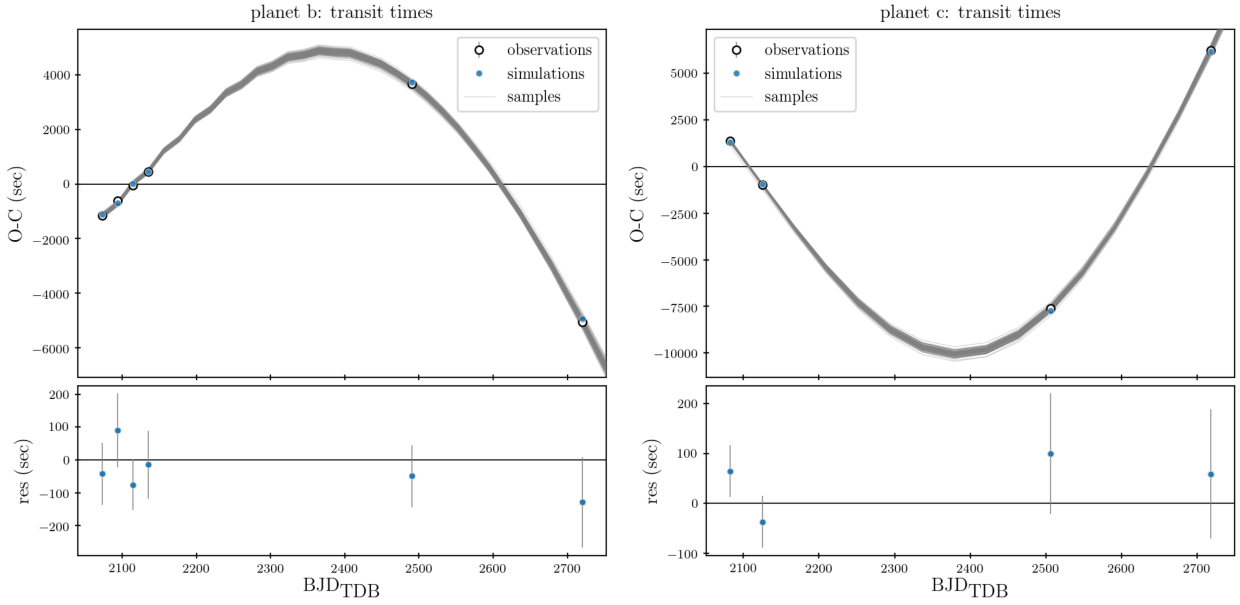


**Fig. 3** Top panel: Observed - Calculated ( $O - C$ ) plot of K2-24 b (left) and c (right) synthetic transit times for the baseline of the observations. The Observed is given by the synthetic  $T_0$ s (open-black dots) or simulated  $T_0$ s (filled-blue dots), while Calculated is given by the  $T_0$ s computed from linear ephemeris (from synthetic  $T_0$ s). The gray lines are 100 drawn from the posterior distribution. Bottom panel: residuals between observed and simulated  $O - C$ . The x-axis is in unit of days, starting from a reference time  $\text{BJD}_{\text{TDB}} - 2454833 = 2071.0$  to match the transit times from [Petigura et al. \(2018\)](#).

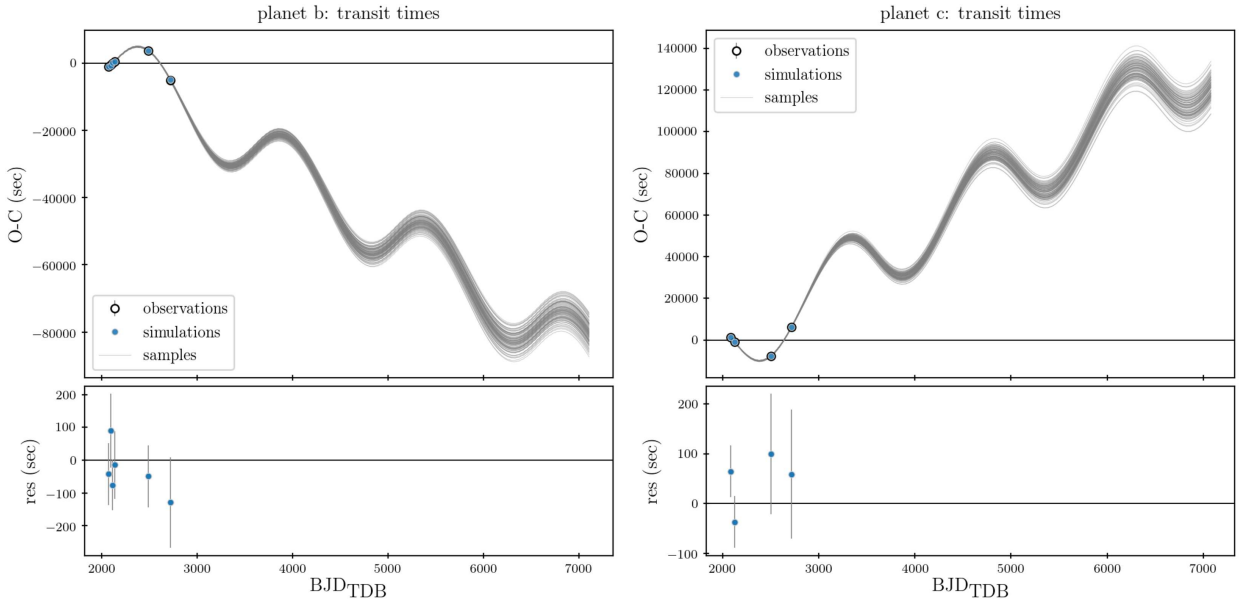


**Fig. 4** Same as Fig. 3, but extending the orbital integration to almost 10 years in the future. The linear trend of the departure from  $O - C = 0$  is due to the short time coverage of the linear ephemeris computed from the synthetic  $T_0$ s.

rameters of the system. This can be easily achieved taking advantage of existing ground-based transit survey, such as the The Asiago Search for Transit timing variations of Exoplanets project (TASTE, [Nascimbeni et al., 2011](#); [Granata et al., 2014](#)), the Next-Generation Transit Survey (NGTS, [Wheatley et al., 2018](#)), and the Ex-

oClock Project<sup>9</sup> (within the *Ariel* Ephemerides Working Group), or space missions, i.e. Transiting Exoplanet Survey Satellite (TESS, [Ricker et al., 2014](#)), CHaracterizing ExOPlanets Satellite (CHEOPS, [Broeg et al., 2014](#); [Benz et al., 2020](#)), PLAnetary Transits and Os-

<sup>9</sup> <https://www.exoclock.space/>

cillations of stars (PLATO, [Rauer et al., 2014](#)). Thanks to TESS and to the extended operations TESS will also be of great advantage for the ephemeris recovery of almost all the *Kepler*/K2 targets on the ecliptic and most of the targets on the sky. With only two transit times from *Ariel* we get an improvement on the uncertainty of the mass of about 22% and 31% for planet b and c, respectively.

### 3.2 Possible TTV signal from *Ariel* observations

In the most favourable case *Ariel* will be able to observe 10 transits of the same planet ([Puig et al., 2018](#); [Tinetti et al., 2018](#)). We wanted to determine the amplitude of the TTV signal ( $A_{\text{TTV}}$ ) produced by an external perturber. We decided to consider as transiting planet the K2-24 b (orbital parameters from [Petigura et al., 2016, 2018](#)) and we used TRADES, by choosing the mass and period of an hypothetical outer perturber from a grid with 30 log-spaced values of mass, ranging from  $1 M_{\oplus}$  to  $4 M_{\text{Nep}}$ , and 30 log-spaced values of orbital period, from 25 to 100 days. For each simulation the code integrates the orbits for 4 years (as the nominal duration of the *Ariel* mission), selects the transit times, with associated error of 35 s determined in Sec. 2.2, and it computes the linear ephemeris. Then it selects 10 random transits (without replacement), re-computes the linear ephemeris, and calculates the  $A_{\text{TTV}}$  as the semi-amplitude of the  $O - C$  (selected transit times minus the newly computed linear ephemeris). It repeats this for 100 times and computes the median of  $A_{\text{TTV}}$ . We obtained a map of the  $A_{\text{TTV}}$  as a function of the mass ( $M_{\text{perturber}}$ ) and of the period ( $P_{\text{perturber}}$ ). It is well known that the eccentricity of the perturber ( $e_{\text{perturber}}$ ) boosts the  $A_{\text{TTV}}$ , so we did the same analysis three times, with three different initial values of  $e_{\text{perturber}}$ : 0.0, 0.05, and 0.1 (see Figures 6, 7, and 8).

The darkest regions of the P-M parameter space (shown in Fig. 5, 6, and 7) where the amplitude  $A_{\text{TTV}}$  is much larger than the timing error  $\sigma_{T_0}$  for the individual transit observations ( $\sim 35$  s, Sec. 2.2) are those where the TTV signal could be detected at high confidence with *Ariel*. At least in some orbital configurations close to a MMR, and especially for eccentric orbits, it will be possible for *Ariel* to robustly detect a TTV signal induced by an outer perturber with one Earth mass (or greater) with just 10 transit observations.

## 4 Conclusions

According to our simulations, the *Ariel* photometric and timing precision is suitable to study known multiple-

planet systems showing TTV signals in order to extend the TTV phase coverage, breaking the degeneracy on the retrieved orbital parameters, and in particular to improve the mass estimation. The latter is fundamental to put strong constraints on planetary formation, migration, and evolution processes (e.g. [Morasini et al., 2012](#)). However, to avoid losing transits within the *Ariel* observing window due to lack of precision on the ephemeris and/or on the orbital parameters, it will be necessary to constrain the ephemeris by taking advantage of ground- (e.g. ExoClock Project, TASTE, and NGTS) and space-based telescopes (e.g. TESS, CHEOPS, and PLATO).

We warn the reader that even if *ArielRad* takes into account different sources of stationary noise and includes a noise margin, it cannot model time-correlated noise. So, we can consider the values of the uncertainty on the  $T_0$  obtained in our analysis as optimistic. As soon as the on-flight performances of the satellite and of instruments will be precisely evaluated we will be able to perform a deeper and more robust analysis of the impact of correlated noise on the determination of the transit time and of its uncertainty. A possible way to model correlated noise (or coloured noise, such as pink and red noise) would be to use non-parametric models such as ARMA or ARIMA processes, creating, for example, a common coloured noise for both FGS1 and FGS2 and an additional coloured noise different for each filter. We want to stress that currently the instrumental correlated noise is unknown and unpredictable and also the stellar noise can vary star-by-star, so it is not so trivial to properly model these noise components.

In the future it would be interesting to repeat the analysis taking into account multiple transits of the same planet observed with *Ariel* (e.g. Tier 3 targets, about  $\sim 10\%$  of Tier 1) and assess the improvement on  $\sigma_{T_0}$ , even if the main contribution derives from the sampling rate of the transit ingress and egress. Furthermore, an MCMC analysis with a different algorithm, such as Nested and Dynamic Nested Sampling ([Skilling, 2004, 2006](#); [Higson et al., 2019](#)) implemented in *dynesty* ([Speagle, 2020](#)) would help to sample in a more efficient and robust way a high dimensional space as in the modelling of many transit light curves in different bands and modelling the dynamics of multi-planet systems.

Furthermore, *Ariel* will be able for some orbital configurations to independently detect TTV signals with about 10 transit observations, allowing us to identify perturbing planets with masses spanning the Earth-Neptune range. Combining RV data with transit times helps to put strong constraints on bulk density and orbital parameters of the transiting planet (e.g. Kepler-



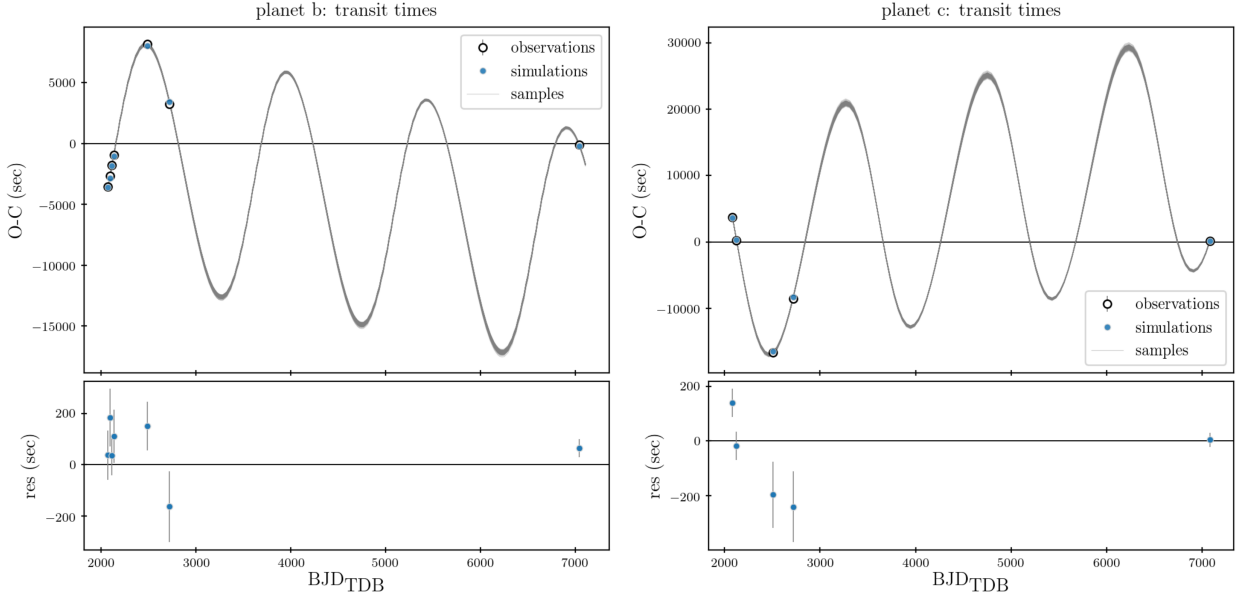


**Fig. 5** Same as Fig. 4, but for the analysis with two  $T_0$ s by *Ariel*, one for planet b (left) and one for planet c (right). The thin gray area is the result of 100 random draws from the posterior distribution; this area is thinner than in Fig. 4 as the result of better determination of orbital parameters.

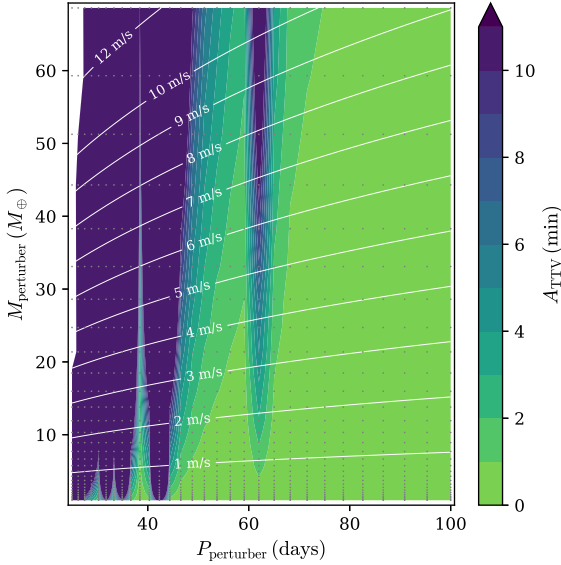


**Fig. 6** TTV amplitude ( $A_{\text{TTV}}$ ) for K2-24 b as a function of mass and period of the perturber. Each gray dot is the combination of mass-period in a grid of 900 simulations, where  $M_{\text{perturber}} = [1 M_{\oplus}, 4 M_{\text{Nep}}]$  and  $P_{\text{perturber}} = [25, 100]$  days, both in 30 logarithmic steps. For each simulation we selected 10 transit times within 4 years of orbital integration, we repeated the selection 100 times and computed the  $A_{\text{TTV}}$  as the median value of the semi-amplitude of the  $O - C$  with respect to a linear ephemeris. In these simulations the initial  $e_{\text{perturber}}$  was set to 0.0. The white contour lines are the RV semi-amplitude due to the perturber.

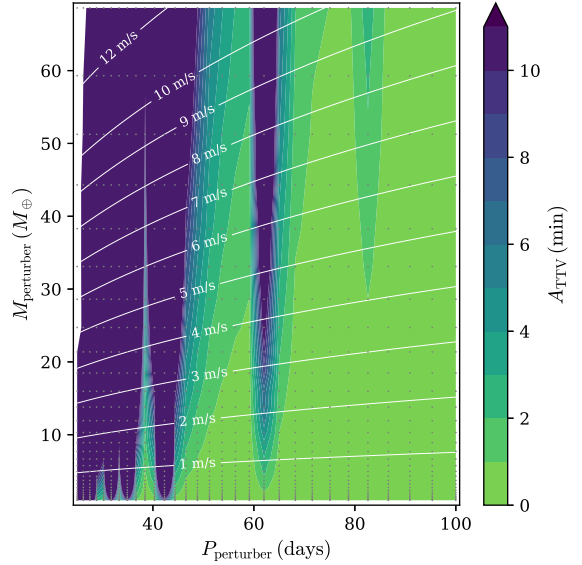


**Fig. 7** Same as Fig. 6, but with initial  $e_{\text{perturber}} = 0.05$ . It is evident that a perturber with non-zero eccentricity extend the possible TTV signal regions and increase their amplitudes.

19 and Kepler-9, Malavolta et al., 2017; Borsato et al., 2019, , respectively). However, if the RV data have not enough precision to detect the external perturber, and taking into account the precision in the mass measurement of 17% for K2-24 c in Petigura et al. (2018), we can say that “in any case” the detection of a TTV signal in *Ariel* data will allow us to determine planetary

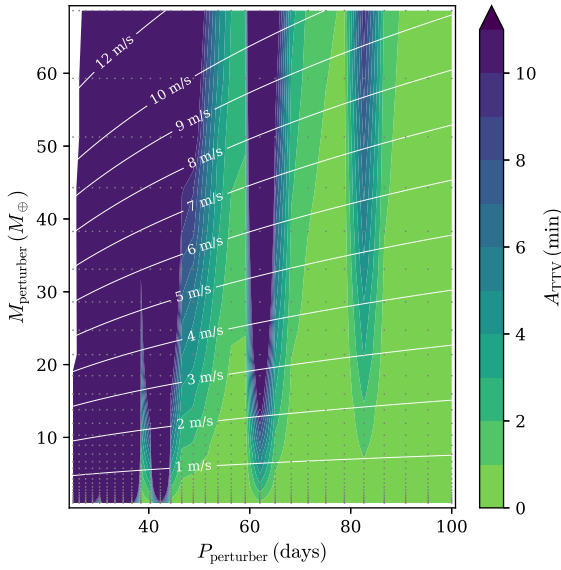


**Fig. 8** Same as Fig. 6, but with initial  $e_{\text{perturber}} = 0.1$ . In this case, the effect of the eccentricity of the perturber is even stronger than that in Fig. 7.

masses of perturber with a precision better than 20% in the Earth-Neptune regime.

The *Ariel* target list is evolving with time and with new discoveries, so at the moment is very difficult to give a quantitative estimates of the number of known multi-planet system with TTV that *Ariel* will observe and characterise. We can expect about several tens of planets with significant TTV improvements, and a similar number of targets with TTV, whose contribution from *Ariel* will be important. Hadden et al. (2019) predicted that about less than 4000 planet systems will be discovered during the nominal mission of TESS and about half of these will be in multi-planet systems. 30 of these multi-planet systems will have a measurable TTV signal and only 10 will be characterised with precise mass measurement from TTV only. Differently from missions like TESS or PLATO, *Ariel* will point a single target, as CHEOPS, and it will observe about 1000 targets, roughly a quarter of the TESS predicted value. So, we can assume for *Ariel* a similar number of the predicted TTV systems for TESS, but only before launch we will know which planets will be observed and how many of these will be systems with TTV, and it will mostly depend on the selection process and on the schedulability of the targets.

**Acknowledgements** LBo, VNa, and GPi acknowledge the funding support from Italian Space Agency (ASI) regulated by “Accordo ASI-INAF n. 2013-016-R.0 del 9 luglio 2013 e integrazione del 9 luglio 2015”.

## References

- Agol E, Steffen J, Sari R, Clarkson W (2005) On detecting terrestrial planets with timing of giant planet transits. *MNRAS* 359(2):567–579, DOI 10.1111/j.1365-2966.2005.08922.x, [2005.08922](#)
- Beichman C, Benneke B, Knutson H, Smith R, Lagage PO, Dressing C, Latham D, Lunine J, Birkmann S, Ferruit P, Giardino G, Kempton E, Carey S, Krick J, Deroo PD, Mandell A, Ressler ME, Shporer A, Swain M, Vasisht G, Ricker G, Bouwman J, Crossfield I, Greene T, Howell S, Christiansen J, Ciardi D, Clampin M, Greenhouse M, Sozzetti A, Goudfrooij P, Hines D, Keyes T, Lee J, McCullough P, Roberto M, Stansberry J, Valenti J, Rieke M, Rieke G, Fortney J, Bean J, Kreidberg L, Ehrenreich D, Deming D, Albert L, Doyon R, Sing D (2014) Observations of Transiting Exoplanets with the James Webb Space Telescope (JWST). *PASP* 126(946):1134, DOI 10.1086/679566
- Benz W, Broeg C, Fortier A, Rando N, Beck T, Beck M, Queloz D, Ehrenreich D, Maxted PFL, Isaak KG, Billot N, Alibert Y, Alonso R, António C, Asquier J, Bandy T, Bárczy T, Barrado D, Barros SCC, Baumjohann W, Bekkelien A, Bergomi M, Biondi F, Bonfils X, Borsato L, Brandeker A, Busch MD, Cabrera J, Cessa V, Charnoz S, Chazelas B, Collier Cameron A, Corral Van Damme C, Cortes D, Davies MB, Deleuil M, Deline A, Delrez L, Demangeon O, Demory BO, Erikson A, Farinato J, Fossati L, Fridlund M, Futyan D, Gandolfi D, Garcia Munoz A, Gillon M, Guterman P, Gutierrez A, Hasiba J, Heng K, Hernandez E, Hoyer S, Kiss LL, Kovacs Z, Kuntzer T, Laskar J, Lecavelier des Etangs A, Lendl M, López A, Lora I, Lovis C, Lüftinger T, Magrin D, Malvasio L, Marafatto L, Michaelis H, de Miguel D, Modrego D, Munari M, Nascimbeni V, Olofsson G, Ottacher H, Ottensamer R, Pagano I, Palacios R, Pallé E, Peter G, Piazza D, Piotto G, Pizarro A, Pollaco D, Ragazzoni R, Ratti F, Rauer H, Ribas I, Rieder M, Rohlfs R, Safa F, Salatti M, Santos NC, Scandariato G, Ségransan D, Simon AE, Smith AMS, Sordet M, Sousa SG, Steller M, Szabó GM, Szoke J, Thomas N, Tschentscher M, Udry S, Van Grootel V, Viotto V, Walter I, Walton NA, Wildi F, Wolter D (2020) The CHEOPS mission. *Experimental Astronomy* DOI 10.1007/s10686-020-09679-4, [2009.11633](#)
- Borsato L, Marzari F, Nascimbeni V, Piotto G, Granata V, Bedin LR, Malavolta L (2014) TRADES: A new software to derive orbital parameters from observed transit times and radial velocities. Revisiting Kepler-11 and Kepler-9. *AAP* 571:A38, DOI 10.1051/0004-6361/201424080, [1408.2844](#)

- Borsato L, Malavolta L, Piotto G, Buchhave LA, Mortier A, Rice K, Collier Cameron A, Coffinet A, Sozzetti A, Charbonneau D, Cosentino R, Dumusque X, Figueira P, Latham DW, Lopez-Morales M, Mayor M, Micela G, Molinari E, Pepe F, Phillips D, Poretti E, Udry S, Watson C (2019) HARPS-N radial velocities confirm the low densities of the Kepler-9 planets. *MNRAS* 484(3):3233–3243, DOI 10.1093/mnras/stz181, [1901.05471](#)
- Borucki WJ, Koch DG, Basri G, Batalha N, Brown TM, Bryson ST, Caldwell D, Christensen-Dalsgaard J, Cochran WD, DeVore E, Dunham EW, Gautier I, Thomas N, Geary JC, Gilliland R, Gould A, Howell SB, Jenkins JM, Latham DW, Lissauer JJ, Marcy GW, Rowe J, Sasselov D, Boss A, Charbonneau D, Ciardi D, Doyle L, Dupree AK, Ford EB, Fortney J, Holman MJ, Seager S, Steffen JH, Tarter J, Welsh WF, Allen C, Buchhave LA, Christiansen JL, Clarke BD, Das S, Désert JM, Endl M, Fabrycky D, Fressin F, Haas M, Horch E, Howard A, Isaacson H, Kjeldsen H, Kolodziejczak J, Kulesa C, Li J, Lucas PW, Machalek P, McCarthy D, MacQueen P, Meibom S, Miquel T, Prsa A, Quinn SN, Quintana EV, Ragozzine D, Sherry W, Shporer A, Tenenbaum P, Torres G, Twicken JD, Van Cleve J, Walkowicz L, Witteborn FC, Still M (2011) Characteristics of Planetary Candidates Observed by Kepler. II. Analysis of the First Four Months of Data. *ApJ* 736(1):19, DOI 10.1088/0004-637X/736/1/19, [1102.0541](#)
- Broeg C, Benz W, Thomas N, Cheops Team (2014) The CHEOPS mission. *Contributions of the Astronomical Observatory Skalnaté Pleso* 43(3):498–498
- Delrez L, Gillon M, Triaud AHMJ, Demory BO, de Wit J, Ingalls JG, Agol E, Bolmont E, Burdakov A, Burgasser AJ, Carey SJ, Jehin E, Leconte J, Lederer S, Queloz D, Selsis F, Van Grootel V (2018) Early 2017 observations of TRAPPIST-1 with Spitzer. *MNRAS* 475(3):3577–3597, DOI 10.1093/mnras/sty051, [1801.02554](#)
- Demory BO, Gillon M, de Wit J, Madhusudhan N, Bolmont E, Heng K, Kataria T, Lewis N, Hu R, Krick J, Stamenković V, Benneke B, Kane S, Queloz D (2016) A map of the large day-night temperature gradient of a super-Earth exoplanet. *Nature* 532(7598):207–209, DOI 10.1038/nature17169, [1604.05725](#)
- Eastman J, Gaudi BS, Agol E (2013) EXOFAST: A Fast Exoplanetary Fitting Suite in IDL. *PASP* 125(923):83, DOI 10.1086/669497, [1206.5798](#)
- Encrenaz T, Tinetti G, Coustenis A (2018) Transit spectroscopy of temperate Jupiters with ARIEL: a feasibility study. *Experimental Astronomy* 46(1):31–44, DOI 10.1007/s10686-017-9561-2
- Espinoza N, Jordán A (2015) Limb darkening and exoplanets: testing stellar model atmospheres and identifying biases in transit parameters. *MNRAS* 450(2):1879–1899, DOI 10.1093/mnras/stv744, [1503.07020](#)
- Foreman-Mackey D, Conley A, Meierjürgen Farr W, Hogg DW, Lang D, Marshall P, Price-Whelan A, Sanders J, Zuntz J (2013) emcee: The MCMC Hammer. [1303.002](#)
- Foreman-Mackey D, Farr W, Sinha M, Archibald A, Hogg D, Sanders J, Zuntz J, Williams P, Nelson A, de Val-Borro M, Erhardt T, Pashchenko I, Plav O (2019) emcee v3: A Python ensemble sampling toolkit for affine-invariant MCMC. *The Journal of Open Source Software* 4(43):1864, DOI 10.21105/joss.01864, [1911.07688](#)
- Goodman J, Weare J (2010) Ensemble samplers with affine invariance. *Communications in Applied Mathematics and Computational Science* 5(1):65–80, DOI 10.2140/camcos.2010.5.65
- Granata V, Nascimbeni V, Piotto G, Bedin LR, Borsato L, Cunial A, Damasso M, Malavolta L (2014) TASTE IV: Refining ephemeris and orbital parameters for HAT-P-20b and WASP-1b. *Astronomische Nachrichten* 335(8):797, DOI 10.1002/asna.201412072, [1405.3288](#)
- Greene TP, Schlawin E, Beichman CA, Line MR, Fortney JJ, Fraine J, JWST NIRCeam Team (2017) Characterizing transiting exoplanet atmospheres using NIRCeam grism spectra. In: *American Astronomical Society Meeting Abstracts #230*, American Astronomical Society Meeting Abstracts, vol 230, p 309.01
- Hadden S, Barclay T, Payne MJ, Holman MJ (2019) Prospects for TTV Detection and Dynamical Constraints with TESS. *AJ* 158(4):146, DOI 10.3847/1538-3881/ab384c, [1811.01970](#)
- Higson E, Handley W, Hobson M, Lasenby A (2019) Dynamic nested sampling: an improved algorithm for parameter estimation and evidence calculation. *Statistics and Computing* 29(5):891–913, DOI 10.1007/s11222-018-9844-0, [1704.03459](#)
- Holczer T, Mazeh T, Nachmani G, Jontof-Hutter D, Ford EB, Fabrycky D, Ragozzine D, Kane M, Steffen JH (2016) Transit Timing Observations from Kepler. IX. Catalog of the Full Long-cadence Data Set. *ApJS* 225(1):9, DOI 10.3847/0067-0049/225/1/9, [1606.01744](#)
- Holman MJ, Murray NW (2005) The Use of Transit Timing to Detect Terrestrial-Mass Extrasolar Planets. *Science* 307(5713):1288–1291, DOI 10.1126/science.1107822, [astro-ph/0412028](#)
- Holman MJ, Fabrycky DC, Ragozzine D, Ford EB, Steffen JH, Welsh WF, Lissauer JJ, Latham DW, Marcy GW, Walkowicz LM, Batalha NM, Jenkins JM, Rowe

- JF, Cochran WD, Fressin F, Torres G, Buchhave LA, Sasselov DD, Borucki WJ, Koch DG, Basri G, Brown TM, Caldwell DA, Charbonneau D, Dunham EW, Gautier TN, Geary JC, Gilliland RL, Haas MR, Howell SB, Ciardi DR, Endl M, Fischer D, Fürész G, Hartman JD, Isaacson H, Johnson JA, MacQueen PJ, Moorhead AV, Morehead RC, Orosz JA (2010) Kepler-9: A System of Multiple Planets Transiting a Sun-Like Star, Confirmed by Timing Variations. *Science* 330(6000):51, DOI 10.1126/science.1195778
- Howell SB, Sobeck C, Haas M, Still M, Barclay T, Mullally F, Troeltzsch J, Aigrain S, Bryson ST, Caldwell D, Chaplin WJ, Cochran WD, Huber D, Marcy GW, Miglio A, Najita JR, Smith M, Twicken JD, Fortney JJ (2014) The K2 Mission: Characterization and Early Results. *PASP* 126(938):398, DOI 10.1086/676406, [1402.5163](#)
- Husser TO, Wende-von Berg S, Dreizler S, Homeier D, Reinert A, Barman T, Hauschildt PH (2013) A new extensive library of PHOENIX stellar atmospheres and synthetic spectra. *AAP* 553:A6, DOI 10.1051/0004-6361/201219058, [1303.5632](#)
- Kipping DM (2010a) Binning is sinning: morphological light-curve distortions due to finite integration time. *MNRAS* 408(3):1758–1769, DOI 10.1111/j.1365-2966.2010.17242.x, [1004.3741](#)
- Kipping DM (2010b) Investigations of approximate expressions for the transit duration. *MNRAS* 407(1):301–313, DOI 10.1111/j.1365-2966.2010.16894.x, [1004.3819](#)
- Kipping DM (2013) Efficient, uninformative sampling of limb darkening coefficients for two-parameter laws. *MNRAS* 435(3):2152–2160, DOI 10.1093/mnras/stt1435, [1308.0009](#)
- Kreidberg L (2015) batman: BASic Transit Model cAlculationN in Python. *PASP* 127(957):1161, DOI 10.1086/683602, [1507.08285](#)
- Kurucz RL (1979) Model atmospheres for G, F, A, B, and O stars. *ApJS* 40:1–340, DOI 10.1086/190589
- Lissauer JJ, Fabrycky DC, Ford EB, Borucki WJ, Fressin F, Marcy GW, Orosz JA, Rowe JF, Torres G, Welsh WF, Batalha NM, Bryson ST, Buchhave LA, Caldwell DA, Carter JA, Charbonneau D, Christiansen JL, Cochran WD, Desert JM, Dunham EW, Fanelli MN, Fortney JJ, Gautier I, Thomas N, Geary JC, Gilliland RL, Haas MR, Hall JR, Holman MJ, Koch DG, Latham DW, Lopez E, McCauliff S, Miller N, Morehead RC, Quintana EV, Ragozzine D, Sasselov D, Short DR, Steffen JH (2011) A closely packed system of low-mass, low-density planets transiting Kepler-11. *Nature* 470(7332):53–58, DOI 10.1038/nature09760, [1102.0291](#)
- Lissauer JJ, Jontof-Hutter D, Rowe JF, Fabrycky DC, Lopez ED, Agol E, Marcy GW, Deck KM, Fischer DA, Fortney JJ, Howell SB, Isaacson H, Jenkins JM, Kolbl R, Sasselov D, Short DR, Welsh WF (2013) All Six Planets Known to Orbit Kepler-11 Have Low Densities. *ApJ* 770(2):131, DOI 10.1088/0004-637X/770/2/131, [1303.0227](#)
- Malavolta L, Borsato L, Granata V, Piotto G, Lopez E, Vanderburg A, Figueira P, Mortier A, Nascimbeni V, Affer L, Bonomo AS, Bouchy F, Buchhave LA, Charbonneau D, Collier Cameron A, Cosentino R, Dressing CD, Dumusque X, Fiorenzano AFM, Harutyunyan A, Haywood RD, Johnson JA, Latham DW, Lopez-Morales M, Lovis C, Mayor M, Micela G, Molinari E, Motalebi F, Pepe F, Phillips DF, Pollacco D, Queloz D, Rice K, Sasselov D, Ségransan D, Sozzetti A, Udry S, Watson C (2017) The Kepler-19 System: A Thick-envelope Super-Earth with Two Neptune-mass Companions Characterized Using Radial Velocities and Transit Timing Variations. *AJ* 153(5):224, DOI 10.3847/1538-3881/aa6897, [1703.06885](#)
- Mazeh T, Nachmani G, Holczer T, Fabrycky DC, Ford EB, Sanchis-Ojeda R, Sokol G, Rowe JF, Zucker S, Agol E, Carter JA, Lissauer JJ, Quintana EV, Ragozzine D, Steffen JH, Welsh W (2013) Transit Timing Observations from Kepler. VIII. Catalog of Transit Timing Measurements of the First Twelve Quarters. *ApJS* 208(2):16, DOI 10.1088/0067-0049/208/2/16, [1301.5499](#)
- Miralda-Escudé J (2002) Orbital Perturbations of Transiting Planets: A Possible Method to Measure Stellar Quadrupoles and to Detect Earth-Mass Planets. *ApJ* 564(2):1019–1023, DOI 10.1086/324279, [astro-ph/0104034](#)
- Mollière P, van Boekel R, Bouwman J, Henning T, Lagage PO, Min M (2017) Observing transiting planets with JWST. Prime targets and their synthetic spectral observations. *AAP* 600:A10, DOI 10.1051/0004-6361/201629800, [1611.08608](#)
- Mordasini C, Alibert Y, Georgy C, Dittkrist KM, Klahr H, Henning T (2012) Characterization of exoplanets from their formation. II. The planetary mass-radius relationship. *AAP* 547:A112, DOI 10.1051/0004-6361/201118464, [1206.3303](#)
- Mugnai LV, Pascale E, Edwards B, Papageorgiou A, Sarkar S (2020) ArielRad: the Ariel radiometric model. *Experimental Astronomy* 50(2-3):303–328, DOI 10.1007/s10686-020-09676-7, [2009.07824](#)
- Nascimbeni V, Piotto G, Bedin LR, Damasso M (2011) TASTE: The Asiago Search for Transit timing variations of Exoplanets. I. Overview and improved parameters for HAT-P-3b and HAT-P-14b. *AAP* 527:A85, DOI 10.1051/0004-6361/201015199, [1011.6395](#)



- Nesvorný D, Kipping D, Terrell D, Hartman J, Bakos GÁ, Buchhave LA (2013) KOI-142, The King of Transit Variations, is a Pair of Planets near the 2:1 Resonance. *ApJ* 777(1):3, DOI 10.1088/0004-637X/777/1/3, [1304.4283](#)
- Pascale E, Bezawada N, Barstow J, Beaulieu JP, Bowles N, Coudé du Foresto V, Coustenis A, Decin L, Drossart P, Eccleston P, Encrenaz T, Forget F, Griffin M, Güdel M, Hartogh P, Heske A, Lagage PO, Leconte J, Malaguti P, Micela G, Middleton K, Min M, Moneti A, Morales JC, Mugnai L, Ollivier M, Pace E, Papageorgiou A, Pilbratt G, Puig L, Rataj M, Ray T, Ribas I, Rocchetto M, Sarkar S, Selsis F, Taylor W, Tennyson J, Tinetti G, Turrini D, Vandenbussche B, Venot O, Waldmann IP, Wolkenberg P, Wright G, Zapatero Osorio MR, Zingales T (2018) The ARIEL space mission. In: *Proc. SPIE , Society of Photo-Optical Instrumentation Engineers (SPIE) Conference Series*, vol 10698, p 106980H, DOI 10.1117/12.2311838
- Perryman M (2018) *The Exoplanet Handbook*
- Petigura EA, Howard AW, Lopez ED, Deck KM, Fulton BJ, Crossfield IJM, Ciardi DR, Chiang E, Lee EJ, Isaacson H, Beichman CA, Hansen BMS, Schlieder JE, Sinukoff E (2016) Two Transiting Low Density Sub-Saturns from K2. *ApJ* 818(1):36, DOI 10.3847/0004-637X/818/1/36, [1511.04497](#)
- Petigura EA, Benneke B, Batygin K, Fulton BJ, Werner M, Krick JE, Gorjian V, Sinukoff E, Deck KM, Mills SM, Deming D (2018) Dynamics and Formation of the Near-resonant K2-24 System: Insights from Transit-timing Variations and Radial Velocities. *AJ* 156(3):89, DOI 10.3847/1538-3881/aaceac, [1806.08959](#)
- Pilbratt G (2019) ARIEL: ESA's Mission to Study the Nature of Exoplanets. In: *AAS/Division for Extreme Solar Systems Abstracts*, AAS/Division for Extreme Solar Systems Abstracts, vol 51, p 503.04
- Price EM, Rogers LA (2014) Transit Light Curves with Finite Integration Time: Fisher Information Analysis. *ApJ* 794(1):92, DOI 10.1088/0004-637X/794/1/92, [1408.4124](#)
- Puig L, Pilbratt G, Heske A, Escudero I, Crouzet PE, de Vogeleer B, Symonds K, Kohley R, Drossart P, Eccleston P, Hartogh P, Leconte J, Micela G, Ollivier M, Tinetti G, Turrini D, Vandenbussche B, Wolkenberg P (2018) The Phase A study of the ESA M4 mission candidate ARIEL. *Experimental Astronomy* 46(1):211–239, DOI 10.1007/s10686-018-9604-3
- Rauer H, Catala C, Aerts C, Appourchaux T, Benz W, Brandeker A, Christensen-Dalsgaard J, Deleuil M, Gizon L, Goupil MJ, Güdel M, Janot-Pacheco E, Mas-Hesse M, Pagano I, Piotto G, Pollacco D, Santos C, Smith A, Suárez JC, Szabó R, Udry S, Adibekyan V, Alibert Y, Almenara JM, Amaro-Seoane P, Eiff MAV, Asplund M, Antonello E, Barnes S, Baudin F, Belkacem K, Bergemann M, Bihain G, Birch AC, Bonfils X, Boisse I, Bonomo AS, Borsa F, Brandão IM, Brocato E, Brun S, Burleigh M, Burston R, Cabrera J, Cassisi S, Chaplin W, Charpinet S, Chiappini C, Church RP, Csizmadia S, Cunha M, Damasso M, Davies MB, Deeg HJ, Díaz RF, Dreizler S, Dreyer C, Eggenberger P, Ehrenreich D, Eigmüller P, Erikson A, Farmer R, Feltzing S, de Oliveira Fialho F, Figueira P, Forveille T, Fridlund M, García RA, Giommi P, Giuffrida G, Godolt M, Gomes da Silva J, Granzer T, Grenfell JL, Grottsch-Noels A, Günther E, Haswell CA, Hatzes AP, Hébrard G, Hekker S, Helled R, Heng K, Jenkins JM, Johansen A, Khodachenko ML, Kislyakova KG, Kley W, Kolb U, Krivova N, Kupka F, Lammer H, Lanza AF, Lebreton Y, Magrin D, Marcos-Arenal P, Marrese PM, Marques JP, Martins J, Mathis S, Mathur S, Messina S, Miglio A, Montalbán J, Montalto M, Monteiro MJPG, Moradi H, Moravveji E, Mordasini C, Morel T, Mortier A, Nascimbeni V, Nelson RP, Nielsen MB, Noack L, Norton AJ, Ofir A, Oshagh M, Ouazzani RM, Pápics P, Parro VC, Petit P, Plez B, Poretti E, Quirrenbach A, Ragazzoni R, Raimondo G, Rainer M, Reese DR, Redmer R, Reffert S, Rojas-Ayala B, Roxburgh IW, Salmon S, Santerne A, Schneider J, Schou J, Schuh S, Schunker H, Silva-Valio A, Silvotti R, Skillen I, Snellen I, Sohl F, Sousa SG, Sozzetti A, Stello D, Strassmeier KG, Švanda M, Szabó GM, Tkachenko A, Valencia D, Van Grootel V, Vauclair SD, Ventura P, Wagner FW, Walton NA, Weingrill J, Werner SC, Wheatley PJ, Zwintz K (2014) The PLATO 2.0 mission. *Experimental Astronomy* 38(1-2):249–330, DOI 10.1007/s10686-014-9383-4, [1310.0696](#)
- Ricker GR, Winn JN, Vanderspek R, Latham DW, Bakos GÁ, Bean JL, Berta-Thompson ZK, Brown TM, Buchhave L, Butler NR, Butler RP, Chaplin WJ, Charbonneau D, Christensen-Dalsgaard J, Clampin M, Deming D, Doty J, De Lee N, Dressing C, Dunham EW, Endl M, Fressin F, Ge J, Henning T, Holman MJ, Howard AW, Ida S, Jenkins J, Jernigan G, Johnson JA, Kaltenegger L, Kawai N, Kjeldsen H, Laughlin G, Levine AM, Lin D, Lissauer JJ, MacQueen P, Marcy G, McCullough PR, Morton TD, Narita N, Paegert M, Palte E, Pepe F, Pepper J, Quirrenbach A, Rinehart SA, Sasselo D, Sato B, Seager S, Sozzetti A, Stassun KG, Sullivan P, Szentgyorgyi A, Torres G, Udry S, Villaseñor J (2014) Transiting Exoplanet Survey Satellite (TESS). In: *Proc. SPIE , Society of Photo-Optical Instrumenta-*



- tion Engineers (SPIE) Conference Series, vol 9143, p 914320, DOI 10.1117/12.2063489, [1406.0151](#)
- Skilling J (2004) Nested Sampling. In: Fischer R, Preuss R, Toussaint UV (eds) *Bayesian Inference and Maximum Entropy Methods in Science and Engineering: 24th International Workshop on Bayesian Inference and Maximum Entropy Methods in Science and Engineering*, American Institute of Physics Conference Series, vol 735, pp 395–405, DOI 10.1063/1.1835238
- Skilling J (2006) Nested sampling for general bayesian computation. *Bayesian Anal* 1(4):833–859, DOI 10.1214/06-BA127, URL <https://doi.org/10.1214/06-BA127>
- Speagle JS (2020) DYNESTY: a dynamic nested sampling package for estimating Bayesian posteriors and evidences. *MNRAS* 493(3):3132–3158, DOI 10.1093/mnras/staa278, [1904.02180](#)
- Szabó R, Szabó GM, Dálya G, Simon AE, Hodosán G, Kiss LL (2013) Multiple planets or exomoons in Kepler hot Jupiter systems with transit timing variations? *AAP* 553:A17, DOI 10.1051/0004-6361/201220132, [1207.7229](#)
- Tinetti G, Drossart P, Eccleston P, Hartogh P, Heske A, Leconte J, Micela G, Ollivier M, Pilbratt G, Puig L, Turrini D, Vandenbussche B, Wolkenberg P, Beaulieu JP, Buchave LA, Ferus M, Griffin M, Guedel M, Justanont K, Lagage PO, Machado P, Malaguti G, Min M, Nørgaard-Nielsen HU, Rataj M, Ray T, Ribas I, Swain M, Szabo R, Werner S, Barstow J, Burleigh M, Cho J, du Foresto VC, Coustenis A, Decin L, Encrenaz T, Galand M, Gillon M, Helled R, Morales JC, Muñoz AG, Moneti A, Pagano I, Pascale E, Piccioni G, Pinfield D, Sarkar S, Selsis F, Tennyson J, Triaud A, Venot O, Waldmann I, Waltham D, Wright G, Amiaux J, Auguères JL, Berthé M, Bezawada N, Bishop G, Bowles N, Coffey D, Colomé J, Crook M, Crouzet PE, Da Peppo V, Sanz IE, Focardi M, Frericks M, Hunt T, Kohley R, Middleton K, Morgante G, Ottensamer R, Pace E, Pearson C, Stamper R, Symonds K, Rengel M, Renotte E, Ade P, Affer L, Alard C, Allard N, Altieri F, André Y, Arena C, Argyriou I, Aylward A, Baccani C, Bakos G, Banaszekiewicz M, Barlow M, Batista V, Bellucci G, Benatti S, Bernardi P, Bézard B, Blecka M, Bolmont E, Bonfond B, Bonito R, Bonomo AS, Brucato JR, Brun AS, Bryson I, Bujwan W, Casewell S, Charnay B, Pestellini CC, Chen G, Ciaravella A, Claudi R, Clédassou R, Damasso M, Damiano M, Danielski C, Deroo P, Di Giorgio AM, Dominik C, Doublier V, Doyle S, Doyon R, Drummond B, Duong B, Eales S, Edwards B, Farina M, Flaccomio E, Fletcher L, Forget F, Fossey S, Fränz M, Fujii Y, García-Piquer Á, Gear W, Geoffray H, Gérard JC, Gesa L, Gomez H, Graczyk R, Griffith C, Grodent D, Guarcello MG, Gustin J, Hamano K, Hargrave P, Hello Y, Heng K, Herrero E, Hornstrup A, Hubert B, Ida S, Ikoma M, Iro N, Irwin P, Jarchow C, Jaubert J, Jones H, Julien Q, Kameda S, Kerschbaum F, Kervella P, Koskinen T, Krijger M, Krupp N, Lafarga M, Landini F, Lellouch E, Leto G, Luntzer A, Rank-Lüftinger T, Maggio A, Maldonado J, Maillard JP, Mall U, Marquette JB, Mathis S, Maxted P, Matsuo T, Medvedev A, Miguel Y, Minier V, Morello G, Mura A, Narita N, Nascimbeni V, Nguyen Tong N, Noce V, Oliva F, Palles E, Palmer P, Pancrazzi M, Papageorgiou A, Parmentier V, Perger M, Petralia A, Pezzuto S, Pierrehumbert R, Pillitteri I, Piotto G, Pisano G, Prisinzano L, Radioti A, Réess JM, Rezac L, Rochetto M, Rosich A, Sanna N, Santerne A, Savini G, Scandariato G, Sicardy B, Sierra C, Sindoni G, Skup K, Snellen I, Sobiecki M, Soret L, Sozzetti A, Stiepen A, Strugarek A, Taylor J, Taylor W, Terenzi L, Tessenyi M, Tsiaras A, Tucker C, Valencia D, Vasisht G, Vazan A, Vilardell F, Vinatier S, Viti S, Waters R, Wawer P, Wawrzaszek A, Whitworth A, Yung YL, Yurchenko SN, Osorio MRZ, Zellem R, Zingales T, Zwart F (2018) A chemical survey of exoplanets with ARIEL. *Experimental Astronomy* 46(1):135–209, DOI 10.1007/s10686-018-9598-x
- Vanderburg A, Becker J, Buchhave LA, Mortier A, Latham DW, Charbonneau D, Lopez-Morales M, HARPS-N Collaboration (2017) Precise Masses in the WASP-47 Multi-Transiting Hot Jupiter System. In: *American Astronomical Society Meeting Abstracts #230*, American Astronomical Society Meeting Abstracts, vol 230, p 402.04
- von Braun K, Boyajian TS, ten Brummelaar TA, Kane SR, van Belle GT, Ciardi DR, Raymond SN, López-Morales M, McAlister HA, Schaefer G, Ridgway ST, Sturmann L, Sturmann J, White R, Turner NH, Farrington C, Goldfinger PJ (2011) 55 Cancri: Stellar Astrophysical Parameters, a Planet in the Habitable Zone, and Implications for the Radius of a Transiting Super-Earth. *ApJ* 740(1):49, DOI 10.1088/0004-637X/740/1/49, [1106.1152](#)
- Weiss LM, Deck KM, Sinukoff E, Petigura EA, Agol E, Lee EJ, Becker JC, Howard AW, Isaacson H, Crossfield IJM, Fulton BJ, Hirsch L, Benneke B (2017) New Insights on Planet Formation in WASP-47 from a Simultaneous Analysis of Radial Velocities and Transit Timing Variations. *AJ* 153(6):265, DOI 10.3847/1538-3881/aa6c29, [1612.04856](#)
- Weiss LM, Fabrycky DC, Agol E, Mills SM, Howard AW, Isaacson H, Petigura EA, Fulton B, Hirsch L, Sinukoff E (2020) The Discovery of the Long-Period, Eccentric Planet Kepler-88 d and System Character-

- ization with Radial Velocities and Photodynamical Analysis. *AJ* 159(5):242, DOI 10.3847/1538-3881/ab88ca, [1909.02427](#)
- Wheatley PJ, West RG, Goad MR, Jenkins JS, Pollacco DL, Queloz D, Rauer H, Udry S, Watson CA, Chazelas B, Eigmüller P, Lambert G, Genolet L, McCormac J, Walker S, Armstrong DJ, Bayliss D, Bento J, Bouchy F, Burleigh MR, Cabrera J, Casewell SL, Chaushev A, Chote P, Csizmadia S, Erikson A, Faedi F, Foxell E, Gänsicke BT, Gillen E, Grange A, Günther MN, Hodgkin ST, Jackman J, Jordán A, Loudén T, Metrailler L, Moyano M, Nielsen LD, Osborn HP, Poppenhaeger K, Raddi R, Raynard L, Smith AMS, Soto M, Titz-Weider R (2018) The Next Generation Transit Survey (NGTS). *MNRAS* 475(4):4476–4493, DOI 10.1093/mnras/stx2836, [1710.11100](#)
- Winn JN (2010) Exoplanet Transits and Occultations, pp 55–77
- Zingales T, Tinetti G, Pillitteri I, Leconte J, Micela G, Sarkar S (2018) The ARIEL mission reference sample. *Experimental Astronomy* 46(1):67–100, DOI 10.1007/s10686-018-9572-7, [1706.08444](#)